



Experimental Pathology Laboratories, Inc. PO Box 169, Sterling, VA 20167-0169
Tel: (703) 471-7060 Fax: (703) 471-8447 Website: www.epl-inc.com

September 17, 2013

Dr. Chad M. Thompson, Study Director
ToxStrategies, Inc.
23501 Cinco Ranch Blvd.
Suite G265
Katy, TX 77494

Dear Dr. Thompson:

Enclosed are an original and one bound copy of the final pathology report for ToxStrategies, Inc., Job # 281261I/13026.01.01, "Quantitative Histopathologic Evaluation of Mouse Duodenum Specimens," (EPL Project Number 928-004).

If you have any questions concerning this report, please do not hesitate to contact me.

Sincerely,

A handwritten signature in blue ink, appearing to read "Jeffrey C. Wolf", is written over a light blue horizontal line.

JEFFREY C. WOLF, DVM, Diplomate, ACVP
Senior Pathologist

JCW/cb
Enclosures



Experimental Pathology Laboratories, Inc.

**TOXSTRATEGIES, INC.
JOB # 281261I/13026.01.01**

PATHOLOGY REPORT

ORIGINAL



Experimental Pathology Laboratories, Inc.

TOXSTRATEGIES, INC.
JOB # 281261I/13026.01.01
EPL PROJECT NUMBER 928-004
(ALSO INCORPORATES DATA FROM 928-001, 928-002, AND 928-003)

QUANTITATIVE HISTOPATHOLOGIC EVALUATION OF
MOUSE DUODENUM SPECIMENS

PATHOLOGY REPORT

Submitted by:

Experimental Pathology Laboratories, Inc.

Street Address:

45600 Terminal Drive
Sterling, VA 20166

Mailing Address:

P.O. Box 169
Sterling, VA 20167-0169

(703) 471-7060

Submitted to:

ToxStrategies, Inc.
Katy, TX 77494

September 17, 2013

FINAL REPORT



TABLE OF CONTENTS

	<u>Page</u>
PATHOLOGY SUMMARY	1
APPENDIX A: FIGURES.....	A-1
APPENDIX B: SPREADSHEETS	
Counts of Aberrant Nuclei and Mitotic Figures Using the Entire Section Method	B-1
Counts of Aberrant Nuclei, Mitotic Figures, and Normal Cells Using the Ten Crypts Per Section Method	B-2
Duodenal Mucosal Areas	B-3

PATHOLOGY SUMMARY



TOXSTRATEGIES, INC.
JOB # 281261I/13026.01.01
EPL PROJECT NUMBERS 928-002 AND 928-003

QUANTITATIVE HISTOPATHOLOGIC EVALUATION OF MOUSE
DUODENUM SPECIMENS

PATHOLOGY REPORT

INTRODUCTION

The purpose of this study was to quantitatively evaluate the presence of aberrant nuclei (micronuclei, apoptotic nuclei, and karyorrhectic nuclei) and mitotic figures in Feulgen's-stained histologic sections of duodenal mucosal epithelium from mice treated orally with sodium dichromate dihydrate (SDD), and to determine the areas of the evaluated villus and crypt regions in those histologic sections.

The experimental design is presented in Table 1:

Sacrifice	Group	SDD Concentration (mg/L)	Number of Mice per Treatment	Aberrant Nuclei and Mitotic Figure Counts	Villus and Crypt Areas
8-Day	1	0	5	5	5 ^a
	2	0.3	5	5	5 ^a
	3	4	5	5	5 ^a
	4	14	5	5	5 ^a
	5	60	5	5	5 ^a
	6	170	5	5	5 ^a
	7	520	5	5	5 ^a
91-Day	1A	0	5	5	5 ^a
	1B	0	5	5	5
	2	0.3	5	5	5
	3	4	5	5	5
	4	14	5	4 ^b	4 ^b
	5	60	5	5	5
	6	170	5	5	5
	7	520	5	5	5 ^a

^a For these animals, villus and crypt areas that had been performed and reported in EPL Project No. 928-001 were re-performed due to the identification of a systemic technical error that affected the original measurements.

^b For one of the mice in this group, the submitted tissue was stomach rather than duodenum; consequently, counts and measurements could not be performed for that animal.

METHODS

The sponsor submitted a total of 225 unstained, paraffin-embedded, transverse sections of duodenum (three sections per mouse) on glass slides to Experimental Pathology Laboratories (EPL®), Inc., Sterling, VA. At EPL, all sections were stained for DNA material using the Feulgen's stain, and covered with glass coverslips.

Systems used to collect and tabulate the image analysis data for this study included: an Olympus® BX51 research microscope enhanced with a 3-axis computer-controlled stepping motorized stage system, focus measurement controller and Z axis limit switch, and a vibration isolation platform (Olympus America, Inc., Melville, NY); a DVC 2000C-00-GE-MGF color digital video camera (Digital Video Camera Company, West Austin, TX, USA); Stereo Investigator software for Design Based Stereology, Image Analysis, and 2D Anatomical Mapping, v. 8.11 (MBF Bioscience, Williston, VT, USA); Image-Pro® Plus (IPP – version 7.0, Media Cybernetics, Silver Spring, Maryland, distributed by Optical Elements Corporation, Dulles, VA); Adobe Photoshop CS v. 8.0 (Adobe Systems Incorporated, San Jose, CA, USA); an IBM-compatible Dell Dimension personal computer running the Microsoft® Windows® XP Professional operating system; and Microsoft® Excel 2003 (Microsoft Corporation). Of these software products, only IPP has been validated in-house according to Good Laboratory Practice guidelines. Unless otherwise stated, image analysis procedures were performed according to methods described in the EPL SOP 18.0. As directed by this document, Image Analysis Project Worksheets (IAPW) were used to record the acquisition and evaluation of digital images.

The components of this project included: 1) counts of aberrant nuclei and mitotic figures in duodenal mucosal epithelial cells, and 2) duodenal mucosal villus and crypt area measurements. Counts of aberrant nuclei and mitotic figures were performed using two methods: 1) the Entire Section Method, and 2) the Ten Crypts Per Section Method.

Using the 40x microscope objective and the Virtual Slice module of the Stereo Investigator software, a montage image (multiple high-resolution images stitched together by the software) was obtained of each Feulgen's-stained section and saved as a TIFF file. A montage image of a grid micrometer that was used for spatial calibration was also acquired using the 40x objective and saved as a TIFF file.

ABERRANT NUCLEI AND MITOTIC FIGURE COUNTS

Entire Section Method

Images were randomized by animal, and the person performing the counts was unaware of the treatment group status of individual animals. Using the IPP software, six different combinations of aberrant nucleus type and location, plus crypt mitotic figures, were differentially counted by virtually marking each nucleus manually via the computer mouse (Appendix A, Fig. 1). The categories were:

- 1) apoptotic nucleus in a crypt [labeled with a red square]
- 2) apoptotic nucleus in a villus [labeled with a blue square]
- 3) karyorrhectic nucleus in a crypt [labeled with a red triangle]
- 4) karyorrhectic nucleus in a villus [labeled with a blue triangle]
- 5) micronucleus in a crypt [labeled with a red circle]
- 6) micronucleus in a villus [labeled with a blue circle]
- 7) mitotic figure in a crypt [labeled with a brown square]

The types of aberrant nuclei to be counted in mucosal epithelial cells and their identification criteria were derived from Goldberg et al., 1983. An **apoptotic nucleus** generally had a smudged, heterochromatic appearance, and a discrete rounding of the cell cytoplasm was often evident (Appendix A, Fig. 2). **Karyorrhectic nuclei** were fragmented into small, unequally-sized, dense spherical bodies, and the cytoplasmic margins of such cells were often indistinct (Appendix A, Fig. 3). Each **micronucleus** consisted of a single dense, ovoid to spherical body that was located adjacent to a normal nucleus within the cytoplasm of the same cell (Appendix A, Fig. 4). A **mitotic figure** had distinctly evident chromosomal components (Appendix A, Fig. 5). Goldberg et al. (1983) additionally described "pyknotic nuclei" as a fourth category of aberrant nuclei, and it was intended initially that pyknotic nuclei would also be counted in the present study. However, during method development it was determined that pyknotic nuclei could not be

identified reliably (it was difficult to distinguish potential pyknotic nuclei from intra-epithelial lymphocytes, for example); thus counting of pyknotic nuclei was not attempted.

The entire mucosal region of each image was evaluated using a virtual grid overlay to facilitate counting. The acquisition of measurements was guided by user-created IPP macro subroutines. Data produced by IPP were exported automatically to a Microsoft Excel spreadsheet for tabulation. All image files, IPP-generated measurement files, and ancillary files (e.g., .tag files) that were produced during the analysis were archived and tabulated electronically. In some instances, images were re-evaluated based on subsequent review by the pathologist. Microsoft Excel worksheets were used to compile the data and perform mean and standard deviation calculations.

Ten Crypts Per Section Method

This method was applied only to mice of the 91-day sacrifice, excluding Group 1A animals. Again, images were randomized by animal, and the person performing the counts was unaware of the treatment group status of individual animals. This time, however, only a single image (the first image in the series) was used for each animal, and only crypts (vs. crypts and villi) were evaluated. Ten full-length crypts were selected arbitrarily in each image. Using the IPP software, three different combinations of aberrant nucleus type, plus crypt mitotic figures and “normal” nuclei, were differentially counted by virtually marking each nucleus manually via the computer mouse (Appendix A, Fig. 6).

The categories were:

- 1) apoptotic nucleus in a crypt [labeled with a red square]
- 2) karyorrhectic nucleus in a crypt [labeled with a red triangle]
- 3) micronucleus in a crypt [labeled with a red circle]
- 4) mitotic figure in a crypt [labeled with a blue circle]
- 5) “normal” nucleus in a crypt [labeled with a brown square]

Data produced by IPP were exported automatically to a Microsoft Excel spreadsheet for tabulation. All image files, IPP-generated measurement files, and

ancillary files (e.g., .tag files) that were produced during the analysis were archived and tabulated electronically. Microsoft Excel worksheets were used to compile the data and perform mean and standard deviation calculations.

DUODENAL AREA MEASUREMENTS

Using the IPP software, two different area measurements were obtained independently per image, and these were: 1) the mucosal area, and 2) the villus area (Appendix A, Figs. 7-9. For each of these areas, the external border was outlined manually using the computer mouse. Conversely, the internal borders of these areas were determined automatically by the software using IPP's "Count/Size" color segmentation tool and user-defined colorimetric criteria, i.e., colorimetric thresholds were selected so that all tissue internal to the outlines would be measured, but all of the white non-tissue areas (such as the intestinal lumen) would be excluded. Provision was also made to manually exclude non-tissue objects (e.g., gut contents) as deemed necessary by the user.

The spatial calibration was verified daily on each day that area measurements were obtained. The acquisition of measurements was facilitated by user-created IPP macro subroutines. Data produced by IPP was exported automatically to a Microsoft Excel spreadsheet for tabulation. All image files, IPP-generated measurement files, and ancillary files (e.g., .scl files) that were produced during the analysis were archived and tabulated electronically. The pathologist reviewed all area measurements. In some instances, images were re-measured based on further review by the pathologist.

The total mucosa area (evaluated) was calculated as the sum of the mucosal areas in each of the three duodenal images per animal. Similarly, the total villus area was calculated as the sum of the villus areas in each of the three duodenal images per animal. A third area, the total crypt area, was calculated as follows:

$$\text{total crypt area } (\mu\text{m}^2) = \text{total mucosa area } (\mu\text{m}^2) - \text{total villus area } (\mu\text{m}^2)$$

A villus to crypt ratio (total villus area / total crypt area) was additionally calculated. Microsoft Excel worksheets were used to compile the data and perform mean and standard deviation calculations.

During subsequent review of the data by the pathologist it was discovered that duodenal image area measurements obtained for EPL Project No. 928-001 were inaccurate due to issues involving the conversion from TIFF to JPEG files; consequently, all of the previous area measurements from Project No. 928-001 were re-evaluated using the original TIFF files.

RESULTS

ABERRANT NUCLEI AND MITOTIC FIGURE COUNTS – ENTIRE SECTION METHOD

Aberrant nuclei count data are summarized in Table 2 and individual animal data are presented in Appendix B-1. Aberrant nuclei data from EPL Project No. 928-001 are included in Table 2 for reference.

For both the 8-day and 91-day sacrifices, aberrant nuclei were generally increased in SDD-treated mice as compared to controls (Groups 1, and 1A and 1B, respectively). The most substantial increases occurred in Groups 6 and 7.

Crypt apoptotic nuclei were by far the most numerous aberrant nuclei identified in this study, and mean numbers of affected cells were substantially higher than controls in mice of treatment Groups 6 and 7 for the 8-day sacrifice, and Groups 5, 6, and 7 for the 91-day sacrifice. For the 91-day sacrifice only, mean numbers of crypt apoptotic nuclei were also slightly higher in groups 2, 3, and 4 compared to controls. For Group 6 mice of the 91-day sacrifice, the standard deviation of the mean was exceptionally high (i.e., the value was greater than the mean itself) due to the inordinately high number of apoptotic nuclei that were counted for Animal No. 6F404 as compared to other Group 6 mice. The mean number of crypt apoptotic cells counted in Animal No. 6F404 was greater than two-fold higher than in any other mouse in the study; in that regard, Animal No. 6F404 could possibly be considered an outlier. In some instances, apoptotic nuclei were difficult to differentiate from

mitotic figures, the most likely reason for which is that cells undergoing mitosis were the most susceptible to apoptotic change.

For both the 8-day and 91-day sacrifices, there were slight increases in the mean numbers of villus micronuclei in mice of Groups 6 and 7 compared to controls (in the 8-day sacrifice only, villus micronuclei were also increased in Group 3 relative to controls). Mean numbers of villus karyorrhectic nuclei were also slightly increased relative to controls in Groups 6 and 7 of the 8-day sacrifice, and in Group 6 of the 91-day sacrifice. For the 91-day sacrifice, the increase in mean numbers of villus karyorrhectic nuclei in Group 7 mice as compared to controls was substantial.

For both sacrifices there were no substantial increases in mean numbers of villus apoptotic nuclei, crypt karyorrhectic nuclei, or crypt micronuclei relative to controls.

For both sacrifices, mean numbers of crypt mitotic figures were substantially higher in Groups 6 and 7 as compared to controls, and slightly higher in Groups 4 and 5 (8-day sacrifice) and Groups 2-5 (91-day sacrifice) relative to controls. These increases generally displayed dose-dependent patterns.

The relatively low number of mitotic figures identified in Group 1A mice of the 91-day sacrifice may be a consequence of the suboptimal tissue section plane that existed for two of the mice in that group.

As a caveat, it should be emphasized that types of aberrant nuclei identified in this study represent morphologic classifications that are based on descriptions and photomicrographs from previously published examples. Ancillary techniques (e.g., immunohistochemistry) would be required to establish the definitive identity of such cell types (e.g., to confirm that "apoptotic nuclei" are truly apoptotic).

Sacrifice	Group	n	Total Apoptotic Nuclei Crypts		Total Apoptotic Nuclei Villi		Total Karyorrhectic Nuclei Crypts		Total Karyorrhectic Nuclei Villi		Total Micronuclei Crypts		Total Micronuclei Villi		Total Mitotic Figures Crypts	
			mean	SD	mean	SD	mean	SD	mean	SD	mean	SD	mean	SD	mean	SD
8-day	1	5	1.6	0.9	0.2	0.4	0.0	0.0	0.0	0.0	0.2	0.4	0.2	0.4	119.8	37.0
	2	5	2.0	1.9	0.0	0.0	0.0	0.0	0.0	0.0	0.0	0.0	0.6	0.9	115.2	47.1
	3	5	1.8	0.8	0.0	0.0	0.0	0.0	0.0	0.0	0.0	0.0	1.0	0.7	111.2	28.4
	4	5	1.2	1.1	0.0	0.0	0.0	0.0	0.0	0.0	0.0	0.0	0.4	0.5	164.0	79.8
	5	5	1.4	1.3	0.6	0.9	0.0	0.0	0.4	0.9	0.0	0.0	0.2	0.4	187.4	68.0
	6	5	5.8	3.3	0.2	0.4	0.0	0.0	0.6	0.5	0.0	0.0	1.2	1.3	268.8	144.2
	7	5	13.4	3.8	0.2	0.4	0.2	0.4	1.8	1.3	0.0	0.0	2.2	3.3	387.0	189.0
91-day	1A	5	0.8	1.3	0.6	1.3	0.0	0.0	0.0	0.0	0.0	0.0	0.2	0.4	60.0	18.0
	1B	5	2.4	1.1	0.8	0.8	0.0	0.0	0.0	0.0	0.4	0.9	0.2	0.4	109.6	20.4
	2	5	3.4	1.8	0.2	0.4	0.2	0.4	0.2	0.4	0.4	0.9	0.2	0.4	145.4	44.0
	3	5	4.6	6.4	0.0	0.0	0.0	0.0	0.0	0.0	0.2	0.4	0.4	0.5	177.2	18.6
	4	4	4.3	3.9	0.0	0.0	0.0	0.0	0.0	0.0	0.3	0.5	0.0	0.0	213.5	110.0
	5	5	7.2	2.2	0.0	0.0	0.2	0.4	1.0	1.4	0.0	0.0	0.4	0.5	244.8	57.5
	6	5	11.8	14.2	0.4	0.5	0.2	0.4	1.2	1.8	0.0	0.0	1.8	1.3	366.8	159.8
	7	5	8.0	3.4	0.0	0.0	0.0	0.0	5.0	4.9	0.0	0.0	1.8	1.5	319.2	28.7

ABERRANT NUCLEI, MITOTIC FIGURE, AND NORMAL CELL COUNTS – TEN CRYPTS PER SECTION METHOD

Aberrant nuclei count data are summarized in Table 3 and individual animal data are presented in Appendix B-2.

Mean numbers of crypt apoptotic nuclei were modestly increased in Group 6 and 7 mice relative to the control group (1B), and also slightly increased in Groups 2, 4, and 5. However, the Apoptotic Index (Total Apoptotic Nuclei Crypts / Grand Total Nuclei Crypts) was only slightly increased in Groups 2, 4, 6, and 7 vs. controls, and these increases did not occur in a dose responsive manner.

Mean numbers of crypt mitotic figures were increased substantially in Groups 4-7 relative to controls, and slightly in Groups 2 and 3. However, the Mitotic Index (Total Mitotic Figures Crypts / Grand Total Nuclei Crypts) was only slightly increased in Groups 2-7 vs. controls, and these increases did not occur in a dose responsive manner.

Mean numbers of “normal” (i.e., non-aberrant and non-mitotic) nuclei, and mean numbers of nuclei overall (Grand Total Nuclei), were increased substantially in the crypts of Group 6 and 7 mice as compared to controls, and were increased modestly in Group 5 mice.

Karyorrhectic nuclei were observed only rarely in crypts (Group 2), and micronuclei were not observed in any of the selected crypts.

Table 3. Aberrant Nuclei and Mitotic Figure Counts: Group Means and Standard Deviations (SD) Using the Ten Crypts Per Section Method																
Sacrifice	Group	n	Total Apoptotic Nuclei Crypts		Total Karyorrhectic Nuclei Crypts		Total Micronuclei Crypts		Total Mitotic Figures Crypts		Total Normal Nuclei Crypts		Grand Total Nuclei Crypts		Apop. Index ^a	Mitot. Index ^b
			mean	SD	mean	SD	mean	SD	mean	SD	mean	SD	mean	SD		
91-day	1B	5	1.8	0.8	0.0	0.0	0.0	0.0	5.6	4.6	376.8	23.9	384.2	25.6	0.47%	1.46%
	2	5	3.4	1.5	0.8	1.3	0.0	0.0	8.0	4.5	329.2	39.3	341.4	43.9	1.00%	2.34%
	3	5	1.8	1.5	0.0	0.0	0.0	0.0	8.6	2.4	354.6	12.6	365.0	10.3	0.49%	2.36%
	4	4	2.5	1.3	0.0	0.0	0.0	0.0	11.0	2.7	341.5	37.2	355.0	40.2	0.70%	2.36%
	5	5	2.4	1.7	0.0	0.0	0.0	0.0	11.4	3.0	463.4	68.4	477.2	68.2	0.50%	2.39%
	6	5	4.6	5.3	0.0	0.0	0.0	0.0	15.2	6.9	529.4	43.0	549.2	48.7	0.84%	2.77%
	7	5	4.2	2.2	0.0	0.0	0.0	0.0	12.6	5.3	622.0	122.5	638.8	118.6	0.66%	1.97%

^aApoptotic Index = Total Apoptotic Nuclei Crypts / Grand Total Nuclei Crypts

^bMitotic Index = Total Mitotic Figures Crypts / Grand Total Nuclei Crypts

DUODENAL AREA MEASUREMENTS

Duodenal area measurement data (group means and standard deviations) are presented in Table 4. Individual animal data are presented in Appendix B-3.

In both the 8-day and 91-day sacrifices, duodenal villus/crypt ratios were decreased substantially in mice of Groups 6 and 7 as compared to controls (Group 1). In both sacrifices, the decreased ratios were driven primarily by increases in mean total crypt area as opposed to changes in mean total villus area. In fact, despite the histologically obvious villus atrophy and collapse in the duodena of Group 6 and 7 mice of both sacrifices, mean total villus areas for these groups were similar to those of controls (Group 6) or only slightly lower than those of controls (Group 7) for mice of the 8-day sacrifice, and were actually greater than those of controls for Group 6 and 7 mice of the 91-day sacrifice.


Morphologically, the increases in crypt area were consistent with elongation of the crypts as a result of mucosal crypt epithelial hyperplasia.

Table 4. Duodenal Area Measurements: Group Means and Standard Deviations (SD)										
Sacrifice	Group	n	Total Mucosa Area (μm^2)		Total Villus Area (μm^2)		Total Crypt Area (μm^2)		Villus / Crypt Ratio	
			mean	SD	mean	SD	mean	SD	mean	SD
8-Day	1	5	5,015,146	722,032	3,501,866	558,894	1,513,280	180,388	2.31	0.18
	2	5	5,409,528	550,020	3,874,039	339,903	1,535,489	233,322	2.55	0.25
	3	5	5,229,707	797,355	3,785,177	590,476	1,444,530	281,384	2.68	0.52
	4	5	4,665,901	830,573	3,390,986	552,817	1,274,916	303,110	2.70	0.33
	5	5	6,662,027	1,174,391	4,856,301	786,093	1,805,726	508,231	2.77	0.52
	6	5	5,853,023	2,510,996	3,675,447	1,776,741	2,177,576	788,592	1.62	0.37
	7	5	5,186,558	1,587,881	2,968,074	947,713	2,218,483	664,535	1.33	0.14
91-Day	1A	5	5,139,102	1,509,969	3,712,020	1,115,290	1,427,082	411,958	2.59	0.29
	1B	5	5,079,328	917,407	3,586,680	680,501	1,492,648	328,701	2.44	0.43
	2	5	6,656,358	1,437,857	4,365,233	793,907	2,291,125	977,847	2.15	0.78
	3	5	4,998,134	993,985	3,732,981	836,140	1,265,153	187,600	2.94	0.41
	4	4	5,733,084	1,171,474	4,120,854	902,697	1,612,229	286,870	2.55	0.21
	5	5	6,614,374	781,051	4,453,908	790,266	2,160,466	104,848	2.07	0.39
	6	5	8,715,458	1,793,004	5,678,689	1,165,199	3,036,769	640,109	1.87	0.08
	7	5	8,334,515	1,258,017	4,777,124	1,235,520	3,557,391	236,130	1.35	0.35

DISCUSSION AND CONCLUSIONS

Although apoptotic nuclei and mitotic figures were increased substantially in the crypts of SDD-treated mice as compared to controls, and especially in Groups 6 and 7 (170 and 520 mg/L, respectively), the overall data suggest that such increases are likely the result of crypt hyperplasia as an indirect proliferative response to damage that occurred primarily in the villus compartment. Villus damage in Group 6 and 7 mice is suggested by: 1) the increased mean number of villus karyorrhectic nuclei and villus micronuclei as compared to controls, and 2) the substantial decrease in the villus/crypt ratio compared to controls. Crypt hyperplasia in Group 6 and 7 mice is supported by: 1) the increase in the mean number of total crypt nuclei as compared to controls, and 2) the increase in total crypt area as compared to controls. Results which suggest that direct damage to the crypt compartment was not a prominent cause of the crypt hyperplasia include: 1) the lack of increased karyorrhectic nuclei and micronuclei in the crypt

epithelium in treated mice as compared to controls, and 2) the lack of a substantial increase in the Apoptotic Index in the crypts of treated mice relative to controls. Thus the increased absolute number of apoptotic crypt cells in treated animals vs. controls may, at least to some extent, been a consequence of the crypt epithelial hyperplasia (i.e., associated with rapid cell turnover); although direct damage to susceptible cells undergoing mitosis cannot be ruled out entirely. A result which suggested that the test article was not in itself mitogenic was the lack of a substantial increase in the Mitotic Index of treated mice relative to controls.



JEFFREY C. WOLF, DVM, Diplomate, ACVP
Senior Pathologist

9-17-13
Date

JCW/cb

REFERENCES

Goldberg MT, Blakey DH, Bruce WR (1983) Comparison of the effects of 1,2-dimethylhydrazine and cyclophosphamide on micronucleus incidence in bone marrow and colon. Mutation Research, 109:91-98.

APPENDIX A
FIGURES

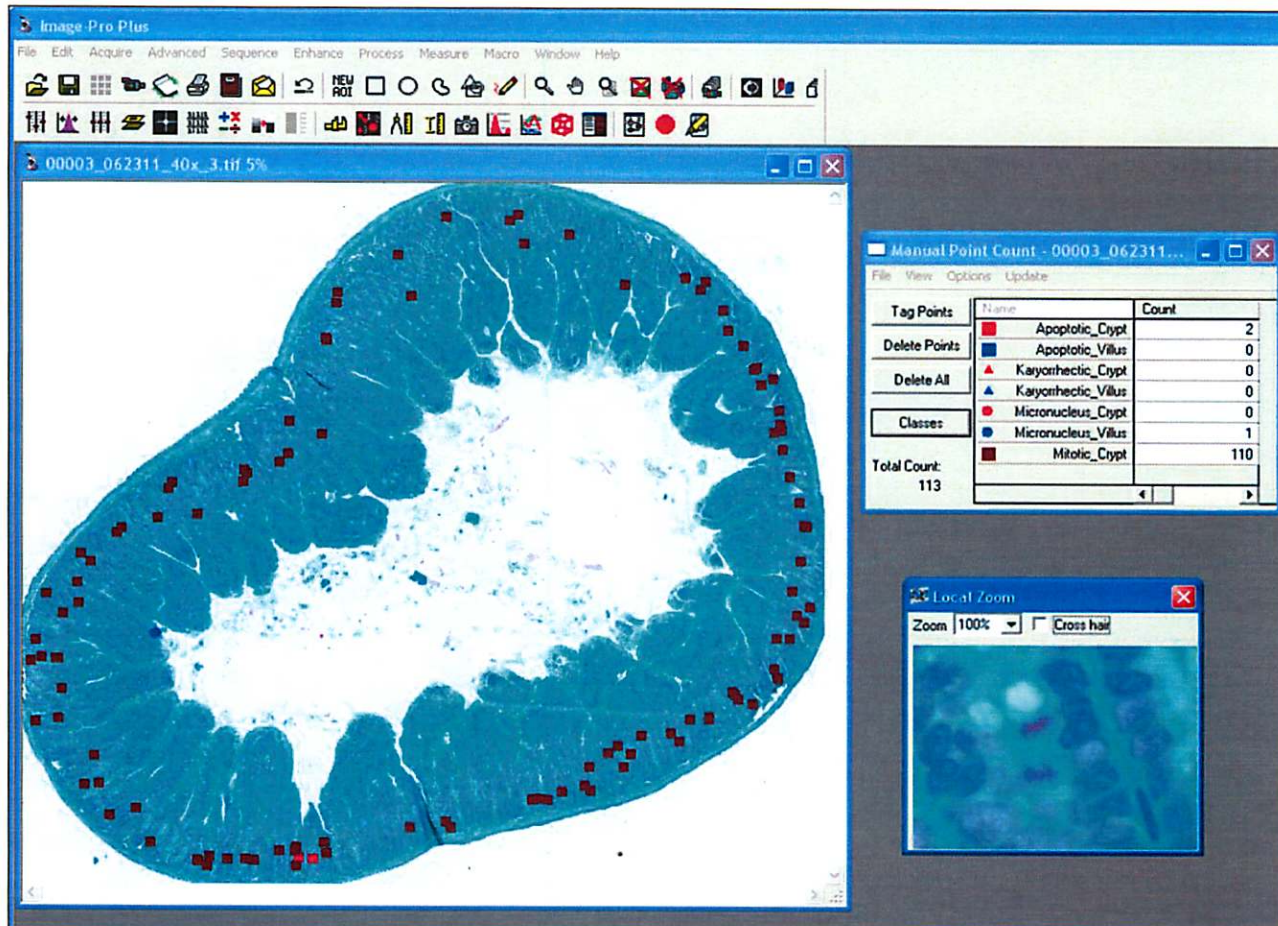


Figure 1. Example of aberrant nuclei and mitotic figure counting in villi and crypts using the IPP software and the Entire Section Method. Counting was performed at a magnification equivalent to, or higher than, that provided by a 40x microscope objective.

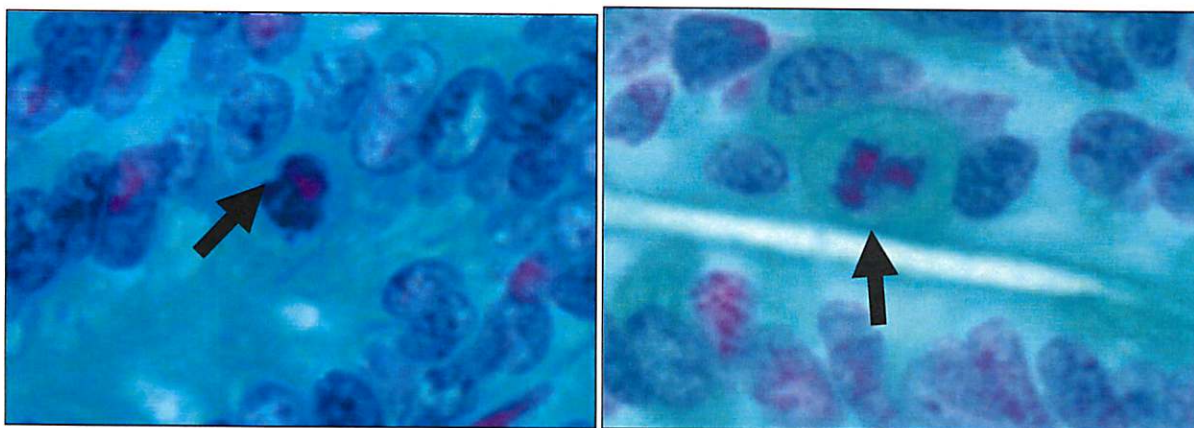


Figure 2. Examples of cells with *apoptotic nuclei* (arrows).

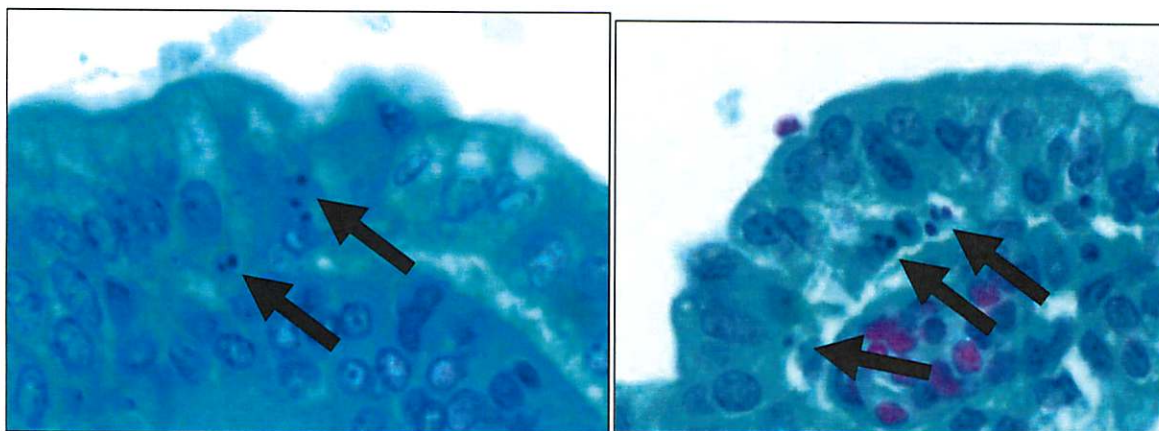


Figure 3. Examples of cells with *karyorrhectic nuclei* (arrows).

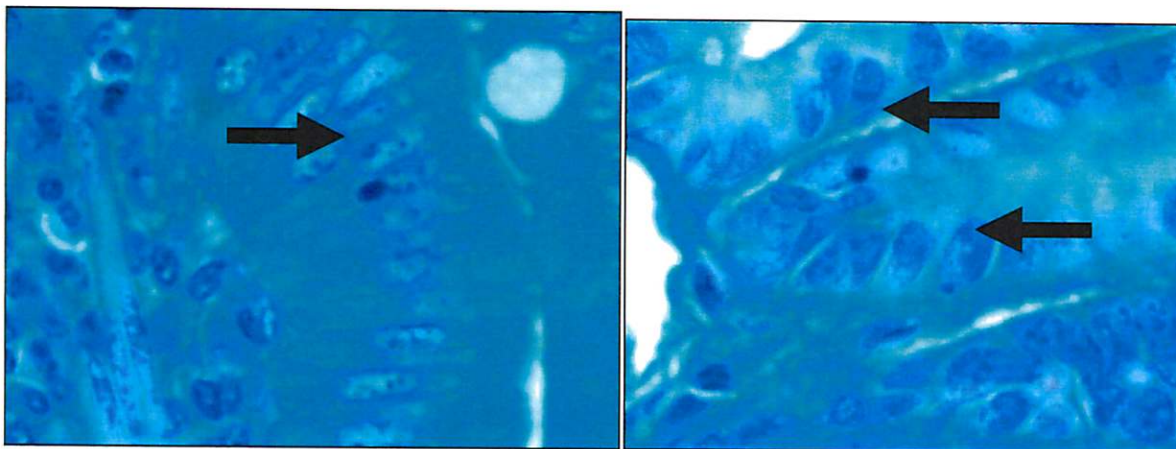


Figure 4. Examples of cells with *micronuclei* (arrows).

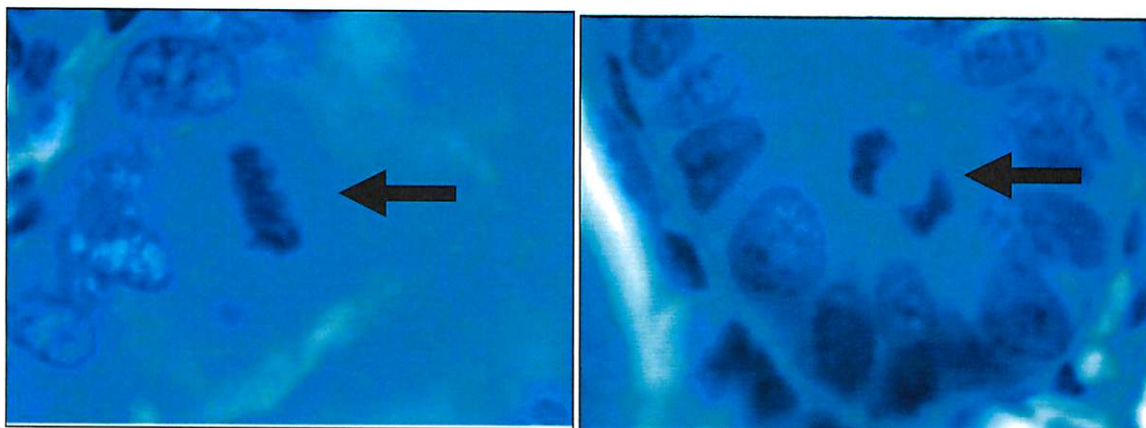


Figure 5. Examples of cells with *mitotic figures* (arrows)

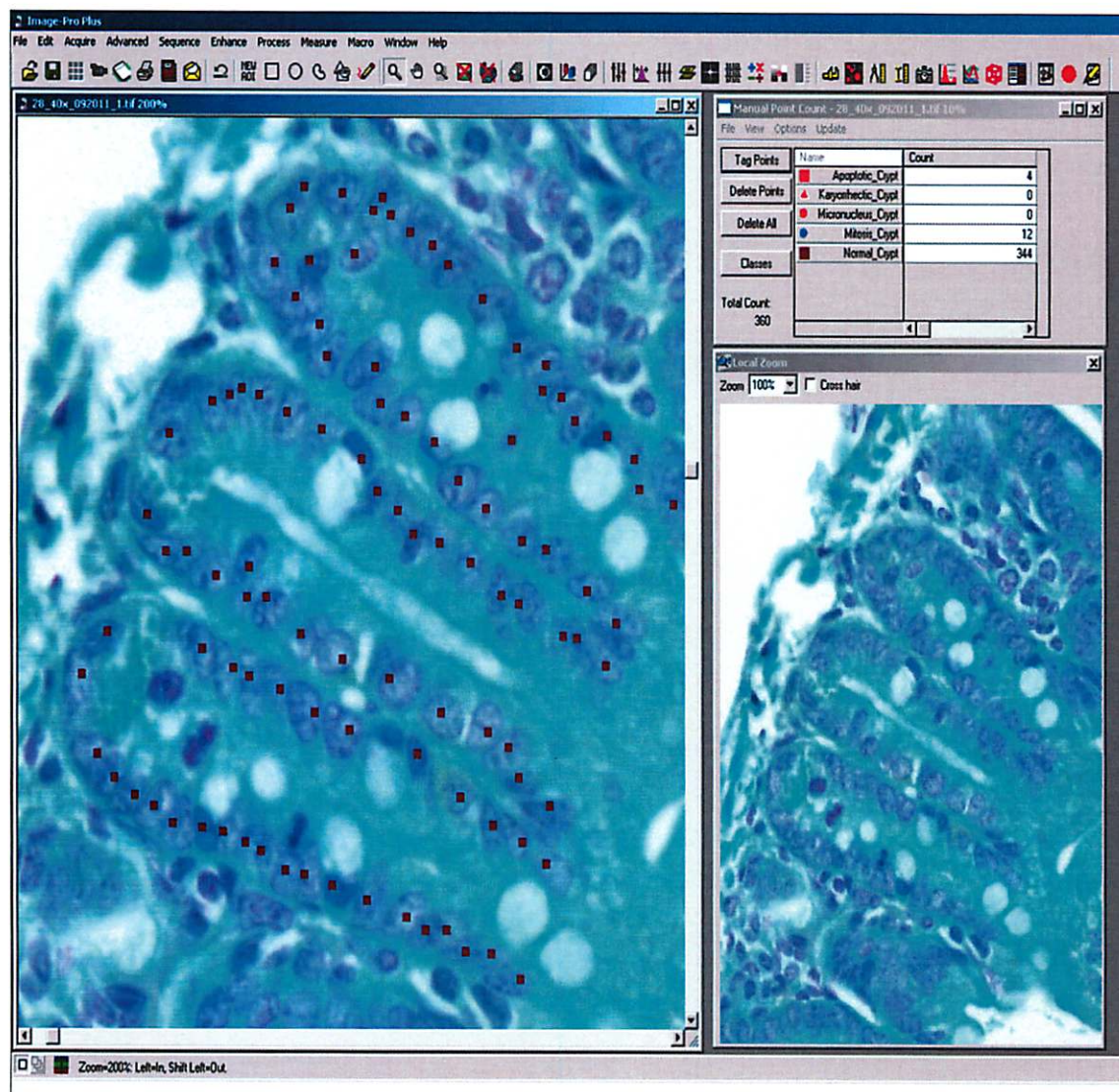


Figure 6. Example of aberrant nuclei, mitotic figure and normal cell counting in crypts using the IPP software and the Ten Crypts Per Section Method. Again, counting was performed at a magnification equivalent to, or higher than, that provided by a 40x microscope objective. Note: all squares in this figure are brown (i.e., normal crypt epithelial cells).

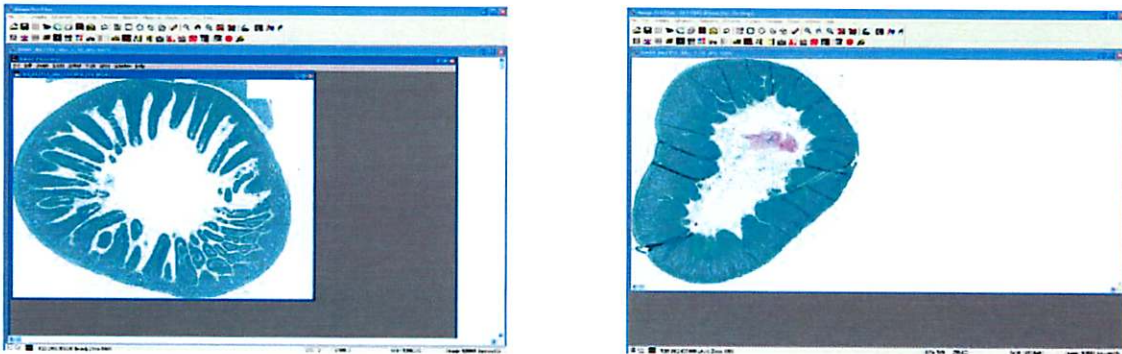


Figure 7. Duodenal sections from 91-day sacrifice mice, Group 1 (left) and Group 7 (right)

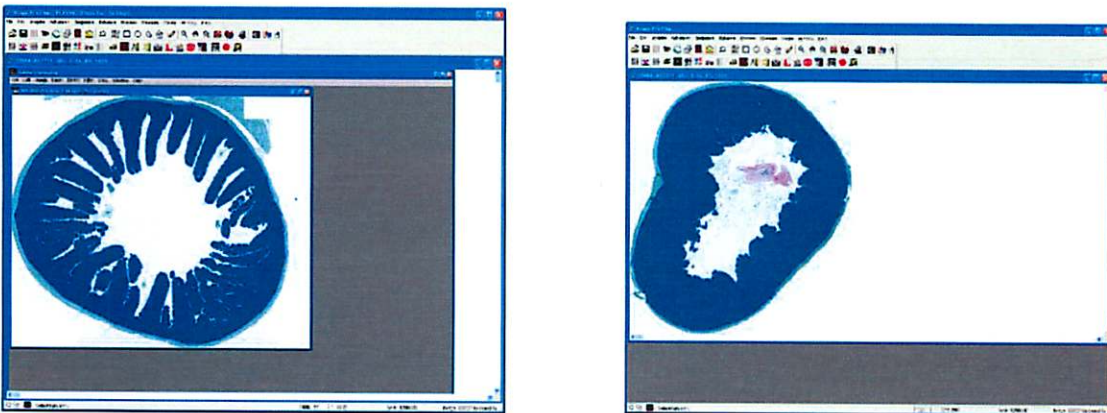


Figure 8. Examples of *mucosal area* measurement (dark blue pseudocolor).

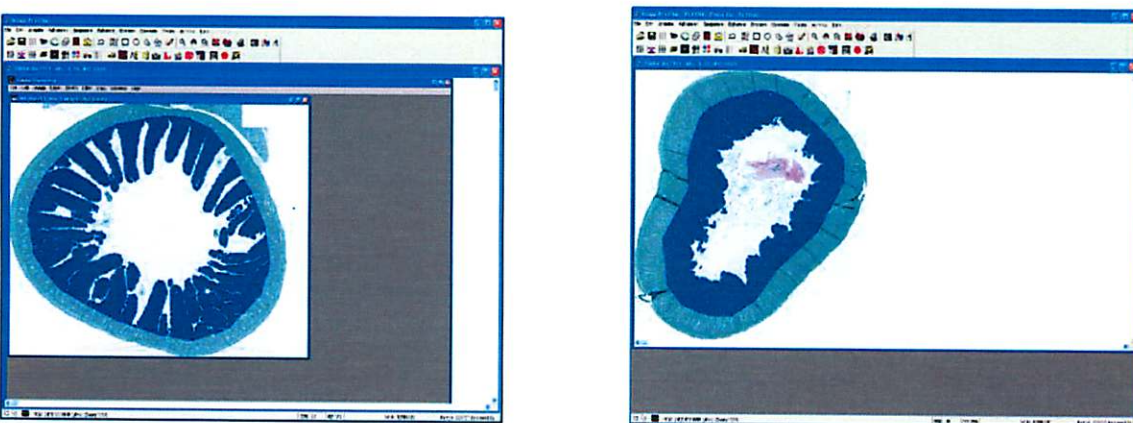


Figure 9. Examples of *villus area* measurement (dark blue pseudocolor).

**APPENDIX B
SPREADSHEETS**

APPENDIX B-1
COUNTS OF ABERRANT NUCLEI AND MITOTIC FIGURES USING
THE ENTIRE SECTION METHOD

ENTIRE SECTION METHOD																								
Animal No.	Sacrifice Day	Treatment Group	Individual Animal Results								Group Means and Standard Deviations													
			Total Apoptotic Crypt	Total Apoptotic Villus	Total Karyorrhectic Crypt	Total Karyorrhectic Villus	Total Micronucleus Crypt	Total Micronucleus Villus	Total Mitotic Crypt	Total Apoptotic Crypt	SD	Total Apoptotic Villus	SD	Total Karyorrhectic Crypt	SD	Total Karyorrhectic Villus	SD	Total Micronucleus Crypt	SD	Total Micronucleus Villus	SD	Total Mitotic Crypt	SD	
1F046	8	1	3	0	0	0	0	0	1	176	1.6	0.9	0.2	0.4	0.0	0.0	0.0	0.2	0.4	0.2	0.4	119.8	37.0	
1F047	8	1	1	0	0	0	0	0	0	121														
1F048	8	1	1	0	0	0	0	1	0	83														
1F049	8	1	1	0	0	0	0	0	0	129														
1F050	8	1	2	1	0	0	0	0	0	90	2.0	1.9	0.0	0.0	0.0	0.0	0.0	0.0	0.0	0.6	0.9	115.2	47.1	
2F126	8	2	4	0	0	0	0	0	1	63														
2F127	8	2	0	0	0	0	0	0	0	190														
2F128	8	2	1	0	0	0	0	2	122															
2F129	8	2	4	0	0	0	0	0	0	106	1.8	0.8	0.0	0.0	0.0	0.0	0.0	0.0	0.0	1.0	0.7	111.2	28.4	
2F130	8	2	1	0	0	0	0	0	0	95														
3F206	8	3	1	0	0	0	0	0	0	85														
3F207	8	3	2	0	0	0	0	0	1	106														
3F208	8	3	2	0	0	0	0	0	1	84	1.2	1.1	0.0	0.0	0.0	0.0	0.0	0.0	0.0	0.4	0.5	164.0	79.8	
3F209	8	3	3	0	0	0	0	0	1	135														
3F210	8	3	1	0	0	0	0	2	146															
4F286	8	4	3	0	0	0	0	0	0	115														
4F287	8	4	1	0	0	0	0	0	0	168	1.4	1.3	0.6	0.9	0.0	0.0	0.4	0.9	0.0	0.0	0.2	0.4	187.4	68.0
4F288	8	4	0	0	0	0	0	0	1	99														
4F289	8	4	1	0	0	0	0	0	0	139														
4F290	8	4	1	0	0	0	0	0	1	299														
5F366	8	5	0	2	0	0	0	0	0	123	5.8	3.3	0.2	0.4	0.0	0.0	0.6	0.5	0.0	0.0	1.2	1.3	268.8	144.2
5F367	8	5	2	0	0	2	0	1	162															
5F368	8	5	2	0	0	0	0	0	0	303														
5F369	8	5	3	1	0	0	0	0	0	174														
5F370	8	5	0	0	0	0	0	0	0	175	13.4	3.8	0.2	0.4	0.2	0.4	1.8	1.3	0.0	0.0	2.2	3.3	387.0	189.0
6F446	8	6	8	0	0	0	0	0	0	308														
6F447	8	6	0	0	0	1	0	0	0	62														
6F448	8	6	6	0	0	1	0	1	220															
6F449	8	6	7	0	0	0	0	2	458	0.8	1.3	0.6	1.3	0.0	0.0	0.0	0.0	0.0	0.0	0.2	0.4	60.0	18.0	
6F450	8	6	8	1	0	1	0	3	296															
7F526	8	7	15	1	0	1	0	2	686															
7F527	8	7	9	0	0	1	0	0	0															233
7F528	8	7	13	0	1	4	0	8	266	2.4	1.1	0.8	0.8	0.0	0.0	0.0	0.0	0.4	0.9	0.2	0.4	109.6	20.4	
7F529	8	7	19	0	0	2	0	1	461															
7F530	8	7	11	0	0	1	0	0	289															
1F001	91	1	0	0	0	0	0	0	0	40	0.8	1.3	0.6	1.3	0.0	0.0	0.0	0.0	0.0	0.0	0.2	0.4	60.0	18.0
1F002	91	1	0	0	0	0	0	0	0	61														
1F003	91	1	3	3	0	0	0	1	54															
1F004	91	1	1	0	0	0	0	0	0	56														
1F005	91	1	0	0	0	0	0	0	0	89	2.4	1.1	0.8	0.8	0.0	0.0	0.0	0.0	0.4	0.9	0.2	0.4	109.6	20.4
1F006	91	1	3	1	0	0	0	0	0	97														
1F007	91	1	2	2	0	0	2	0	143															
1F008	91	1	2	0	0	0	0	0	0	94														
1F009	91	1	4	0	0	0	0	0	1	99	3.4	1.8	0.2	0.4	0.2	0.4	0.2	0.4	0.4	0.9	0.2	0.4	145.4	44.0
1F010	91	1	1	1	0	0	0	0	0	115														
2F081	91	2	1	0	0	0	0	0	0	87														
2F082	91	2	6	1	1	0	2	0	141															
2F083	91	2	4	0	0	0	0	0	0	153	4.6	6.4	0.0	0.0	0.0	0.0	0.0	0.0	0.2	0.4	0.4	0.5	177.2	18.6
2F084	91	2	3	0	0	0	0	0	0	136														
2F085	91	2	3	0	0	1	0	1	210															
3F161	91	3	16	0	0	0	0	0	0	169														
3F162	91	3	1	0	0	0	0	0	1	176	4.3	3.9	0.0	0.0	0.0	0.0	0.0	0.0	0.3	0.5	0.0	0.0	213.5	110.0
3F163	91	3	3	0	0	0	0	0	0	188														
3F164	91	3	1	0	0	0	0	0	0	201														
3F165	91	3	2	0	0	0	1	1	152	7.2	2.2	0.0	0.0	0.2	0.4	1.0	1.4	0.0	0.0	0.4	0.5	244.8	57.5	
4F241	91	4	7	0	0	0	1	0	345															
4F243	91	4	8	0	0	0	0	0	262															
4F244	91	4	0	0	0	0	0	0	139															
4F245	91	4	2	0	0	0	0	0	108	11.8	14.2	0.4	0.5	0.2	0.4	1.2	1.8	0.0	0.0	1.8	1.3	366.8	159.8	
5F321	91	5	6	0	1	0	0	1	272															
5F322	91	5	6	0	0	2	0	1	269															
5F323	91	5	6	0	0	0	0	0	307															
5F324	91	5	7	0	0	0	0	0	180	8.0	3.4	0.0	0.0	0.0	0.0	5.0	4.9	0.0	0.0	1.8	1.5	319.2	28.7	
5F325	91	5	11	0	0	3	0	0	216															
6F401	91	6	3	0	0	4	0	3	385															
6F402	91	6	5	0	0	0	0	1	261															
6F403	91	6	7	0	0	0	0	0	305	8.0	3.4	0.0	0.0	0.0	0.0	5.0	4.9	0.0	0.0	1.8	1.5	319.2	28.7	
6F404	91	6	37	1	1	2	0	2	247															
6F405	91	6	7	1	0	0	0	3	636															
7F481	91	7	7	0	0	1	0	0	349															
7F482	91	7	8	0	0	5	0	2	338	8.0	3.4	0.0	0.0	0.0	0.0	5.0	4.9	0.0	0.0	1.8	1.5	319.2	28.7	
7F483	91	7	3	0	0	1	0	1	326															
7F484	91	7	10	0	0	5	0	2	276															
7F485	91	7	12	0	0	13	0	4	307															

APPENDIX B-2
COUNTS OF ABERRANT NUCLEI, MITOTIC FIGURES, AND NORMAL CELLS USING
THE TEN CRYPTS PER SECTION METHOD

Animal No.	Sacrifice Day	Treatment Group	Individual Animal Results						Group Means and Standard Deviations													
			Apoptotic Crypt	Karyorrhectic Crypt	Micronucleus Crypt	Mitoses Crypt	Normal Crypt	Total Crypt Cells	Apoptotic Crypt	SD	Karyorrhectic Crypt	SD	Micronucleus Crypt	SD	Mitoses Crypt	SD	Normal Crypt	SD	Total Crypt Cells	SD	Apoptotic Index	Mitotic Index
1F006	91	1B	3	0	0	2	384	389	1.8	0.8	0.0	0.0	0.0	0.0	5.6	4.6	376.8	23.9	384.2	25.6	0.47%	1.46%
1F007	91	1B	1	0	0	11	402	414														
1F008	91	1B	2	0	0	1	346	349														
1F009	91	1B	2	0	0	4	394	400														
1F010	91	1B	1	0	0	10	358	369	3.4	1.5	0.8	1.3	0.0	0.0	8.0	4.5	329.2	39.3	341.4	43.9	1.00%	2.34%
2F081	91	2	1	0	0	7	299	307														
2F082	91	2	4	3	0	9	379	395														
2F083	91	2	5	0	0	6	290	301														
2F084	91	2	3	0	0	3	316	322	1.8	1.5	0.0	0.0	0.0	8.6	2.4	354.6	12.6	365.0	10.3	0.49%	2.36%	
2F085	91	2	4	1	0	15	362	382														
3F161	91	3	4	0	0	12	344	360														
3F162	91	3	0	0	0	6	375	381														
3F163	91	3	1	0	0	7	352	360	2.5	1.3	0.0	0.0	0.0	11.0	2.7	341.5	37.2	355.0	40.2	0.70%	2.36%	
3F164	91	3	2	0	0	8	345	355														
3F165	91	3	2	0	0	10	357	369														
4F241	91	4	4	0	0	15	392	411														
4F243	91	4	3	0	0	10	316	329	2.4	1.7	0.0	0.0	0.0	11.4	3.0	463.4	68.4	477.2	68.2	0.50%	2.39%	
4F244	91	4	2	0	0	10	311	323														
4F245	91	4	1	0	0	9	347	357														
5F321	91	5	3	0	0	12	461	476														
5F322	91	5	1	0	0	7	412	420	4.6	5.3	0.0	0.0	0.0	15.2	6.9	529.4	43.0	549.2	48.7	0.84%	2.77%	
5F323	91	5	1	0	0	15	421	437														
5F324	91	5	2	0	0	10	581	593														
5F325	91	5	5	0	0	13	442	460														
6F401	91	6	1	0	0	13	509	523	4.2	2.2	0.0	0.0	0.0	12.6	5.3	622.0	122.5	638.8	118.6	0.66%	1.97%	
6F402	91	6	3	0	0	13	485	501														
6F403	91	6	3	0	0	14	523	540														
6F404	91	6	14	0	0	9	530	553														
6F405	91	6	2	0	0	27	600	629	4.2	2.2	0.0	0.0	0.0	12.6	5.3	622.0	122.5	638.8	118.6	0.66%	1.97%	
7F481	91	7	3	0	0	12	496	511														
7F482	91	7	2	0	0	7	796	805														
7F483	91	7	3	0	0	19	526	548														
7F484	91	7	6	0	0	8	688	702														
7F485	91	7	7	0	0	17	604	628														

APPENDIX B-3
DUODENAL MUCOSAL AREAS

Animal No.	Sacrifice Day	Treatment Group	Individual Animal Results				Group Means and Standard Deviations							
			Total Mucosa Area (µm²)	Total Villus Area (µm²)	Total Crypt Area (µm²)	Villus / Crypt Ratio	Total Mucosa Area (µm²)	SD	Total Villus Area (µm²)	SD	Total Crypt Area (µm²)	SD	Villus / Crypt Ratio	SD
1F046	8	1	5,329,728	3,824,648	1,505,080	2.54	5,015,146	722,032	3,501,866	558,894	1,513,280	180,388	2.31	0.18
1F047	8	1	5,448,206	3,732,059	1,716,148	2.17								
1F048	8	1	4,223,474	2,874,531	1,348,943	2.13								
1F049	8	1	4,271,948	2,949,147	1,322,801	2.23								
1F050	8	1	5,802,373	4,128,943	1,673,430	2.47	5,409,528	550,020	3,874,039	339,903	1,535,489	233,322	2.55	0.25
2F126	8	2	5,445,644	3,777,540	1,668,104	2.26								
2F127	8	2	5,811,113	4,078,685	1,732,428	2.35								
2F128	8	2	5,949,484	4,277,862	1,671,622	2.56								
2F129	8	2	4,547,837	3,376,379	1,171,458	2.88	5,229,707	797,355	3,785,177	590,476	1,444,530	281,384	2.68	0.52
2F130	8	2	5,293,564	3,859,730	1,433,834	2.69								
3F206	8	3	4,466,101	3,476,501	989,600	3.51								
3F207	8	3	5,420,502	3,850,283	1,570,219	2.45								
3F208	8	3	5,711,349	4,182,942	1,528,408	2.74	4,665,901	830,573	3,390,986	552,817	1,274,916	303,110	2.70	0.33
3F209	8	3	6,193,841	4,458,088	1,735,753	2.57								
3F210	8	3	4,356,740	2,958,072	1,398,668	2.11								
4F286	8	4	4,365,917	3,205,164	1,160,753	2.76								
4F287	8	4	5,071,817	3,776,578	1,295,240	2.92	6,662,027	1,174,391	4,856,301	786,093	1,805,726	508,231	2.77	0.52
4F288	8	4	4,033,294	2,848,664	1,184,630	2.40								
4F289	8	4	3,937,836	2,976,416	961,420	3.10								
4F290	8	4	5,920,643	4,148,107	1,772,536	2.34								
5F366	8	5	6,915,727	5,328,232	1,587,495	3.36	5,853,023	2,510,996	3,675,447	1,776,741	2,177,576	788,592	1.62	0.37
5F367	8	5	6,698,700	5,093,285	1,605,415	3.17								
5F368	8	5	8,353,788	5,646,060	2,707,728	2.09								
5F369	8	5	6,229,790	4,579,276	1,650,515	2.77								
5F370	8	5	5,112,128	3,634,653	1,477,475	2.46	5,186,558	1,587,881	2,968,074	947,713	2,218,483	664,535	1.33	0.14
6F446	8	6	8,440,191	5,625,357	2,614,834	2.23								
6F447	8	6	1,795,880	1,001,513	794,367	1.26								
6F448	8	6	7,095,910	4,393,889	2,702,020	1.63								
6F449	8	6	5,468,565	3,178,152	2,290,413	1.39	5,079,328	917,407	3,586,680	680,501	1,492,648	328,701	2.44	0.43
6F450	8	6	6,464,568	3,978,324	2,486,244	1.60								
7F526	8	7	6,187,004	3,334,434	2,852,570	1.17								
7F527	8	7	5,526,085	3,265,819	2,260,265	1.44								
7F528	8	7	6,293,348	3,743,333	2,550,015	1.47	5,139,102	1,509,969	3,712,020	1,115,290	1,427,082	411,958	2.59	0.29
7F529	8	7	5,504,439	3,179,213	2,325,226	1.37								
7F530	8	7	2,421,913	1,317,571	1,104,342	1.19								
1F001	91	1A	2,782,768	1,911,340	871,428	2.19								
1F002	91	1A	5,487,699	4,100,297	1,387,402	2.96	5,079,328	917,407	3,586,680	680,501	1,492,648	328,701	2.44	0.43
1F003	91	1A	6,931,941	4,904,053	2,027,887	2.42								
1F004	91	1A	4,923,414	3,560,433	1,362,980	2.61								
1F005	91	1A	5,569,689	4,083,979	1,485,710	2.75								
1F006	91	1B	5,025,371	3,482,016	1,543,355	2.26	6,656,358	1,437,857	4,365,233	793,907	2,291,125	977,847	2.15	0.78
1F007	91	1B	5,770,137	3,814,475	1,955,662	1.95								
1F008	91	1B	3,583,519	2,481,890	1,101,628	2.25								
1F009	91	1B	5,134,599	3,868,832	1,265,768	3.06								
1F010	91	1B	5,883,013	4,286,186	1,596,827	2.68	4,998,134	993,985	3,732,981	836,140	1,265,153	187,600	2.94	0.41
2F081	91	2	6,987,127	3,649,214	3,337,912	1.09								
2F082	91	2	8,950,181	5,583,625	3,366,557	1.66								
2F083	91	2	5,554,117	3,846,727	1,707,390	2.25								
2F084	91	2	5,382,844	4,016,217	1,366,628	2.94	5,733,084	1,171,474	4,120,854	902,697	1,612,229	286,870	2.55	0.21
2F085	91	2	6,407,520	4,730,382	1,677,138	2.82								
3F161	91	3	4,395,060	3,179,200	1,215,860	2.61								
3F162	91	3	4,981,931	3,844,315	1,137,615	3.38								
3F163	91	3	4,250,573	3,009,863	1,240,709	2.43	6,614,374	781,051	4,453,908	790,266	2,160,466	104,848	2.07	0.39
3F164	91	3	6,705,051	5,114,287	1,590,764	3.21								
3F165	91	3	4,658,057	3,517,238	1,140,818	3.08								
4F241	91	4	7,028,355	5,186,329	1,842,026	2.82								
4F243	91	4	6,222,265	4,452,465	1,769,800	2.52	8,715,458	1,793,004	5,678,689	1,165,199	3,036,769	640,109	1.87	0.08
4F244	91	4	5,392,169	3,756,574	1,635,596	2.30								
4F245	91	4	4,289,546	3,088,050	1,201,495	2.57								
5F321	91	5	6,742,831	4,752,520	1,990,311	2.39								
5F322	91	5	7,067,914	4,823,967	2,243,947	2.15	8,334,515	1,258,017	4,777,124	1,235,520	3,557,391	236,130	1.35	0.35
5F323	91	5	7,603,242	5,420,668	2,182,573	2.48								
5F324	91	5	5,885,030	3,639,947	2,245,082	1.62								
5F325	91	5	5,772,852	3,632,437	2,140,415	1.70								
6F401	91	6	7,884,996	5,129,513	2,755,483	1.86	7,789,166	4,535,823	3,253,344	1,39				
6F402	91	6	7,739,459	5,038,076	2,701,383	1.86								
6F403	91	6	6,805,856	4,414,698	2,391,159	1.85								
6F404	91	6	9,996,400	6,670,441	3,325,958	2.01								
6F405	91	6	11,150,581	7,140,719	4,009,863	1.78	8,334,515	1,258,017	4,777,124	1,235,520	3,557,391	236,130	1.35	0.35
7F481	91	7	8,035,464	4,142,377	3,893,087	1.06								
7F482	91	7	7,517,850	4,079,108	3,438,742	1.19								
7F483	91	7	10,560,948	6,963,950	3,596,997	1.94								
7F484	91	7	7,769,147	4,164,363	3,604,784	1.16								
7F485	91	7	7,789,166	4,535,823	3,253,344	1.39								